Non-Gaussian dynamics of a dilute hard-sphere gas

T. Yamaguchi[a] and Y. Kimura
Department of Chemistry, Graduate School of Science, Kyoto University, Kyoto 606-8502, Japan

(Received 23 October 2000; accepted 20 November 2000)

We have calculated nonlinear time correlation functions of a dilute hard-sphere gas numerically by using the Monte Carlo method, to find that the single particle dynamics in a dilute hard-sphere gas does not follow the Gaussian process. The deviation of the self-part of the dynamic structure factor from a Gaussian function is observed. This non-Gaussian character corresponds to those of Lennard-Jones liquids reported by Itagaki *et al.* [K. Itagaki, M. Goda, and H. Yamada, Physica A **265**, 97 (1999)], if we scale the time unit by the collision frequency. Further, we trapped a particle in a harmonic well and calculated the time development of its distribution, in order to clarify the effect of collisions to the solvation dynamics. Both the Gaussian and the linear response assumptions are broken, and the deviation becomes larger as the curvature of the harmonic well gets larger. © *2001 American Institute of Physics.* [DOI: 10.1063/1.1340616]

I. INTRODUCTION

It is one of the central problems in solution chemistry to understand the static and the dynamic solvent fluctuations felt by a solute molecule. Since solvent molecules have so many degrees of freedom ($\sim 10^{23}$), fluctuations are usually assumed to belong to the Gaussian process due to the central limiting theorem. However, some phenomena have been reported that are not explained by the Gaussian statistics.

Tominaga and Yoshihara measured the vibrational dephasing rates of overtones of chloroform by a time-resolved higher-order nonlinear Raman spectroscopy.[1] They found that the decay curves of response functions were exponential, and the vibrational quantum number dependence of dephasing rates is smaller than quadratic. The exponential decay means that the system is in the fast modulation limit, while quadratic quantum number dependence is expected in the fast modulation limit under Gaussian statistics.

It has been known that the self-part of the dynamic structure factor $[F_s(\mathbf{r},t)]$ of liquid argon does not to follow a Gaussian distribution at the time of ps order.[2] Itagaki *et al.* recently calculated the shape of $F_s(\mathbf{r},t)$ of a Lennard-Jones liquid and a molten salt in detail for longer time scale by molecular dynamics (MD) simulations and discussed the non-Gaussian character.[3] From the definition, $F_s(\mathbf{r},t)$ is the distribution of the displacement of a tagged particle between the time interval of $[0,t]$ that is defined by

$$\delta\mathbf{r}(t)\equiv\mathbf{r}(t)-\mathbf{r}(0)=\mathbf{v}(0)t+\int_0^t dt'\int_0^{t'} dt''\,\mathbf{F}(t''), \tag{1}$$

where $\mathbf{r}(t)$, $\mathbf{v}(t)$, and $\mathbf{F}(t)$ stand for the position, velocity, and force from other particles of the tagged particle, respectively. The sum (or integral) of Gaussian processes should be a Gaussian process. Since $\mathbf{v}(0)$ obeys a Gaussian distribution (Maxwell distribution), non-Gaussian character of $\delta\mathbf{r}(t)$ means that $\mathbf{F}(t)$ is not a Gaussian process. The same discussion works in the generalized Langevin formalism, where the non-Gaussian distribution of $\delta\mathbf{r}(t)$ means the non-Gaussian character of the random force.

Nishiyama and Okada measured hole-burning spectra of several dyes in solution, and compared the relaxation profile of the peak and the width of transient holes.[4] They found that the relaxation of the width is slower than that of the peak. The relaxation function of the peak position approximately represents the averaged transition energy, which is defined theoretically as follows:

$$\rho_e^{(\mathrm{ne})}(t)\equiv\frac{\langle\delta U(t)\rangle_{\mathrm{ne}}}{\langle\delta U(0)\rangle_{\mathrm{ne}}}, \tag{2}$$

where δU stands for the deviation of the transition energy from the equilibrium average, and $\langle\cdots\rangle_{\mathrm{ne}}$ means the nonequilibrium average. The relaxation function of the width can be defined in a similar way as follows:

$$\rho_w^{(\mathrm{ne})}(t)\equiv\frac{\langle(\delta U(t)-\langle\delta U(t)\rangle_{\mathrm{ne}})^2\rangle_{\mathrm{ne}}-\langle(\delta U-\langle\delta U\rangle_{\mathrm{eq}})^2\rangle_{\mathrm{eq}}}{\langle(\delta U(0)-\langle\delta U(0)\rangle_{\mathrm{ne}})^2\rangle_{\mathrm{ne}}-\langle(\delta U-\langle\delta U\rangle_{\mathrm{eq}})^2\rangle_{\mathrm{eq}}}. \tag{3}$$

Both nonequilibrium averages are approximated by the equilibrium time correlation functions $[\rho_e^{(\mathrm{eq})}(t)$ and $\rho_w^{(\mathrm{eq})}(t)]$ within the linear response assumption in the following way:

$$\rho_e^{(\mathrm{ne})}(t)\cong\rho_e^{(\mathrm{eq})}(t)\equiv\frac{\langle\delta U(0)\,\delta U(t)\rangle}{\langle(\delta U)^2\rangle}, \tag{4}$$

$$\rho_w^{(\mathrm{ne})}(t)\cong\rho_w^{(\mathrm{eq})}(t)\equiv\frac{\langle(\delta U(0))^2(\delta U(t))^2\rangle-\langle(\delta U)^2\rangle^2}{\langle(\delta U(0))^4\rangle-\langle(\delta U)^2\rangle^2}, \tag{5}$$

where $\langle\cdots\rangle$ stands for the equilibrium average. The following relationship for $\delta U(t)$ is expected if $\delta U(t)$ is a Gaussian process:

$$\langle(\delta U(0))^2(\delta U(t))^2\rangle=2\langle\delta U(0)\,\delta U(t)\rangle^2+\langle(\delta U)^2\rangle^2. \tag{6}$$

The above equation relates $\rho_e^{(\mathrm{eq})}(t)$ and $\rho_w^{(\mathrm{eq})}(t)$ as follows:

[a]Present address: Institute for Chemical Research, Kyoto University, Gokasho, Uji, Kyoto, 611-0011, Japan.
Electronic mail: tyama@nmr.kuicr.kyoto-u.ac.jp

 © 2001 American Institute of Physics

Downloaded 06 Mar 2008 to 130.54.110.22. Redistribution subject to AIP license or copyright; see http://jcp.aip.org/jcp/copyright.jsp

$$\rho_w^{(\mathrm{eq})}(t)=(\rho_e^{(\mathrm{eq})}(t))^2. \tag{7}$$

Therefore, if the corresponding relationship does not hold between $\rho_e^{(\mathrm{ne})}(t)$ and $\rho_w^{(\mathrm{ne})}(t)$, either the linear response assumption or the Gaussian approximation is broken.

In the previous article, one of us proposed that the collisional character of the solvent fluctuation felt by a solute molecule is a candidate for the origin of non-Gaussian dynamics,[5] which can explain the subquadratic quantum number dependence of the vibrational overtone dephasing rates reported by Tominaga and Yoshihara. In this work, we examine a possibility whether the non-Gaussian character of the binary collision between solute and solvent explains other non-Gaussian processes mentioned above. The collisional effect on the non-Gaussian diffusion was already studied mathematically in momentum space.[6] In the case of rotational diffusion, collision-induced non-Gaussian relaxation appears in angular space as the difference between the *J*-extended diffusion model and the Fokker–Planck–Langevin model.[7,8] However, so far as we know, this is the first application of the collision-induced non-Gaussian process to solvation dynamics in liquids. We consider a dilute hard sphere gas as a model system due to the following two reasons. The first is that we can neglect many-body effects such as correlated collisions. The second is that the idea of ''collision'' exists undoubtedly in the hard-sphere system. At first, we calculate the non-Gaussian parameter (defined in the next section) for the self-diffusion of dilute hard-sphere gas. The non-Gaussian character of the liquid state is qualitatively reproduced in this model. Next, in order to simulate ''solvation dynamics'' in a dilute hard-sphere gas, we trap a tagged particle in a harmonic well and follow the distribution of the tagged particle. The harmonic well corresponds to the free energy surface, and the motion of the tagged particle is regarded as the motion along the solvation coordinate. The solvent motion along the solvation coordinate is perturbed by the collision with other solvent molecules in this model. When the characteristic frequency of the harmonic well is large, the relaxation of the time correlation function of the distribution width is slower than that of the averaged energy. In addition, the nonequilibrium relaxation of the distribution width is found to depend strongly on the initial position.

II. MODELS AND NUMERICAL METHODS

The system under consideration is composed of hard-sphere molecules, whose number density, mass, and diameter are ρ, m, and σ, respectively. The solute (tagged particle) and the solvent (other particles) are assumed to have the same mass and the same radius. Since the length is scaled by $\rho\sigma^2$ in the low-density limit, we can reduce the entire units so that $\rho\sigma^2$, m, and k_BT (Boltzmann constant×temperature) are unity. The molecular chaos assumption holds in the low-density limit, that is, the equilibrium distribution (Maxwell velocity distribution) of solvent molecules is not perturbed by the history of the solute motion. Under this assumption, we can express the probability that a solute of velocity $\mathbf{v}$ collides with a solvent, and that the velocity of the solute increases by $d\mathbf{v}$ in a unit time $[P_c(\mathbf{v},d\mathbf{v})]$ as follows:[9]

$$P_c(\mathbf{v},d\mathbf{v})=\frac{\rho\sigma^2}{\sqrt{2\pi k_BT|d\mathbf{v}|^2/m}}\exp\left[-\frac{m\{(\mathbf{v}+d\mathbf{v})\cdot d\mathbf{v}\}^2}{2k_BT|d\mathbf{v}|^2}\right]. \tag{8}$$

A Monte Carlo method (in the sense of numerical analysis) was employed in order to calculate time correlation functions of a tagged particle. Random walks in the momentum space were generated to follow the transition probability of Eq. (8), and averages of the trajectories were calculated. The initial velocity of a tagged particle was determined to obey the Maxwell distribution. The details of the numerical implementation are given in the Appendix. The numbers of trajectories were 2×10^6 and 1×10^6 for velocity auto correlation function and the self-part of the dynamic structure factor, respectively,

We have also studied the time development of the probability distribution of a tagged particle in a three-dimensional harmonic well $[V(\mathbf{r})]$ as follows:

$$V(\mathbf{r})=\frac{\omega^2|\mathbf{r}|^2}{2}. \tag{9}$$

The frequencies of the well (ω) are 1, 3, and 5. The first one belongs to the overdamped case, and the last one belongs to the underdamped case. The harmonic potential $V(\mathbf{r})$ acts only on a tagged particle, and the other particles move freely except for the time of collisions with each other. We have performed both equilibrium and nonequilibrium runs. Both the initial position and the initial velocity were determined to obey the equilibrium Gaussian distribution in the equilibrium runs. In the nonequilibrium runs, the initial position $[\mathbf{r}(0)]$ was fixed as $(x_0,0,0)$, and the initial velocity follows Maxwell distribution. The values of x_0 were determined so that x_0/ω equals 0, 1, 2, and 3. We regard the *x*-coordinate as the solvation coordinate. Therefore, we substitute x for δU in Eqs. (2)–(7). The number of trajectories was 10^5 except for the calculation of the functional form of the distribution (Fig. 7), where 2×10^5 trajectories were averaged.

III. RESULTS AND DISCUSSION

A. Free particle

We will discuss non-Gaussian character of the motion of a tagged free particle in a dilute hard-sphere gas. First, we show in Fig. 1 the normalized velocity autocorrelation function. The motion of a tagged particle in the dilute gas is known to be described well by the Enskog theory, which predicts that the velocity autocorrelation function decays in a single exponential way, and the time constant (τ_E) can be calculated analytically. In the case of the hard-sphere gas, the value of τ_E is equal to $3/(8\sqrt{\pi})=0.211\,57$. The prediction of the Enskog theory is also shown in Fig. 1. Although the numerical result deviates upward slightly, the agreement with the Enskog theory is good. We also show the time correlation function of the *fluctuation* of the kinetic energy (squared translational velocity) defined as follows:

$$\frac{\langle(\mathbf{v}^2(0)-\langle\mathbf{v}^2\rangle)(\mathbf{v}^2(t)-\langle\mathbf{v}^2\rangle)\rangle}{\langle(\mathbf{v}^2-\langle\mathbf{v}^2\rangle)^2\rangle}. \tag{10}$$

Downloaded 06 Mar 2008 to 130.54.110.22. Redistribution subject to AIP license or copyright; see http://jcp.aip.org/jcp/copyright.jsp

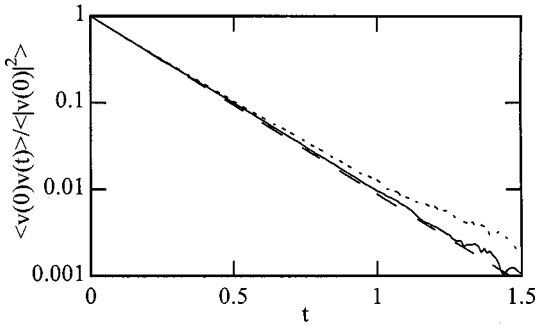

FIG. 1. Velocity autocorrelation functions. Solid and broken curves mean the numerical result and the Enskog theory, respectively. Dotted curve is the time correlation function of the kinetic energy fluctuation defined as Eq. (10).

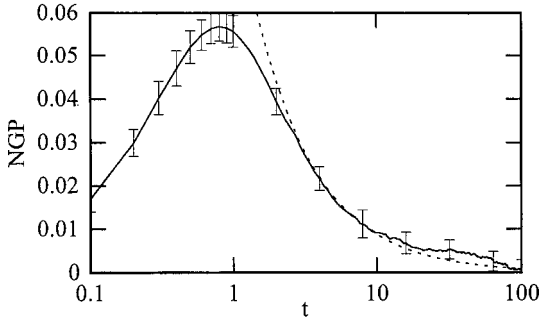

FIG. 3. Time development of the non-Gaussian parameter (NGP) of the self-part of the dynamic structure factor defined as Eq. (11) (solid curve). The *x*-axis is a log-scale. The t^{-1} time profile is also shown by a broken curve.

The decay of the kinetic energy fluctuation is similar to the velocity auto correlation function in the short-time scale, and the upward deviation is found at the long-time. It appears quite natural that the fluctuation of the kinetic energy decays at the same time constant as that of the velocity auto correlation function, since both kinetic energy and translational momentum relax through collisions with solvent molecules. However, the time correlation function of the fluctuation of velocity power to $n(\mathbf{v}^n)$ should decay n times faster than linear velocity auto correlation function, that is, the decay rate of kinetic energy [Eq. (10)] would be twice as large as that of velocity autocorrelation function, if the velocity obeys the Gaussian process. Therefore, this result clearly indicates $\mathbf{v}(t)$ is not a Gaussian process, although the instantaneous distribution of $\mathbf{v}(t)$ is always Gaussian (Maxwell–Boltzmann distribution), which was confirmed both analytically and numerically. Since all relaxation processes are limited by the collision frequency in collisional systems, Gaussian approximation is not appropriate for relaxation processes comparable to the collision frequency.

In Fig. 2, we show the mean-square displacement of a tagged particle. The prediction of the Enskog theory is also shown. The diffusion coefficient from this calculation (D) is slightly larger than that from the Enskog theory ($D_E = 3/(8\sqrt{\pi}) = 0.211\,57$), although both values are very close to each other. The value of D/D_E from this calculation is 1.0183 ± 0.0008. The Enskog theory is not an exact, but an approximated theory, and there are some higher-order theories to correct the Enskog theory.[10] For example, D/D_E equals $59/58 = 1.0172$ by Chapman and Cowling, and $57/56 = 1.0179$ by Kihara. The result of our calculation is close to the values of these theories. When the random force felt by a solute particle follows the Gauss–Markov statistics, the velocity autocorrelation function must be exponential, and the Enskog theory holds exactly.[11] Therefore, the deviation of the diffusion coefficient from the Enskog value stands for the non-Gauss–Markovian nature of the transition probability described by Eq. (8).

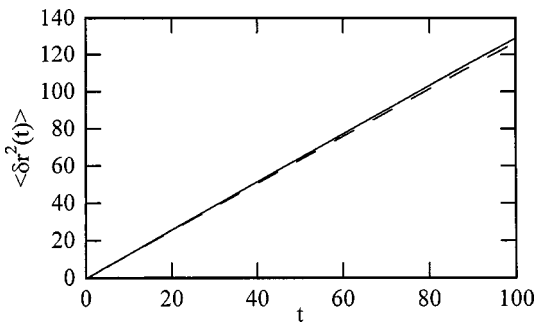

FIG. 2. Mean-square displacement. Solid and broken curves mean the numerical result and the Enskog theory, respectively.

We also studied the non-Gaussian character of the self-part of the dynamic structure factor. For this purpose, we calculated the time development of the non-Gaussian parameter (NGP) as is the case of Itagaki *et al.*[3] The definition of NGP in three-dimensional systems is given by the following expression:

$$\mathrm{NGP} = \frac{3\langle |\delta\mathbf{r}(t)|^4 \rangle}{5\langle |\delta\mathbf{r}(t)|^2 \rangle^2} - 1. \tag{11}$$

The value of NGP indicates how much the distribution deviates from the Gaussian one, since the value of NGP is equal to zero for the Gaussian distribution.

We show in Fig. 3 the time development of NGP. Although it is not shown in the figure, NGP converges to zero as t approaches zero. The value of NGP also approaches zero in the long-time limit due to the central limiting theorem. However, NGP has nonzero values at the intermediate time, as is reported by Rahman[2] and Itagaki *et al.*[3] for Lennard-Jones (LJ) liquid and molten AgI. The non-Gaussian character remains up to $t = 100$, about 500 times larger than the Enskog collision time (τ_E). The time dependence of NGP is close to that of liquid argon reported by Itagaki *et al.* if we regard our time unit as 1 ps. Since the collision frequency in liquid is an order of 100 fs, we consider that this scaling of time unit is reasonable. Therefore, we consider that the collisional dynamics can be a reason for the non-Gaussian motion in liquids, and that the liquid state dynamics has inherited its non-Gaussian character from the collisional dynamics of gases. The time profile of t^{-1} is also shown in Fig. 3. As is seen in the figure, the asymptotic form of NGP is proportional to t^{-1} within the error of our numerical calculation. Considering that NGP is a ratio of fourth-order cumulant to the squared second-order cumulant essentially, t^{-1} decay of

Downloaded 06 Mar 2008 to 130.54.110.22. Redistribution subject to AIP license or copyright; see http://jcp.aip.org/jcp/copyright.jsp

NGP is quite natural from the view of the central limiting theorem. The velocity of the tagged particle loses its memory after the interval longer than τ_E. Since the value of $\delta r(t)$ is the accumulation of the velocity of the tagged particle, $\delta r(t)$ can be regarded as the sum of individual stochastic variables whose number is proportional to t in the case of large t. The central limiting theorem predicts that the ratio of the fourth-order cumulant to the squared second-order one approaches zero as inversely proportional to the number of individual stochastic processes,[12] which means the t^{-1} decay of NGP. The t^{-1} decay is quite a slow relaxation process, and the relaxation time diverges if we define the relaxation time by time integration. In this sense, there is an ultraslow relaxation process in normal liquids (and in gases, too).

B. Tagged particle in a harmonic well

In the first part of this subsection, we show equilibrium time correlation functions that correspond to peak and width. Since we regard the x-coordinate of a tagged particle as the solvation coordinate, the functional forms of $\rho_e^{(\mathrm{eq})}(t)$ and $\rho_w^{(\mathrm{eq})}(t)$ [Eqs. (4) and (5)] are described as follows:

$$\rho_e^{(\mathrm{eq})}(t)=\frac{\langle x(0)x(t)\rangle}{\langle x^2\rangle}=\frac{\omega^2}{3}\langle \mathbf{r}(0)\cdot\mathbf{r}(t)\rangle, \tag{12}$$

$$\rho_w^{(\mathrm{eq})}(t)=\frac{\langle x^2(0)x^2(t)\rangle-\langle x^2\rangle^2}{\langle x^4\rangle-\langle x^2\rangle^2}=\frac{\langle x^2(0)x^2(t)\rangle-\omega^{-4}}{2\omega^{-4}}. \tag{13}$$

In addition to the time correlation function of the *one-dimensional* distribution as described by Eq. (13), we also calculated the time correlation function of the three-dimensional distribution $[\rho_{w3}^{(\mathrm{eq})}(t)]$ defined as follows:

$$\rho_{w3}^{(\mathrm{eq})}(t)\equiv\frac{\langle|\mathbf{r}(0)|^2|\mathbf{r}(t)|^2\rangle-\langle|\mathbf{r}|^2\rangle^2}{\langle|\mathbf{r}|^4\rangle-\langle|\mathbf{r}|^2\rangle^2}=\frac{\langle|\mathbf{r}(0)|^2|\mathbf{r}(t)|^2\rangle-9\omega^{-4}}{6\omega^{-4}}. \tag{14}$$

We show $[\rho_e^{(\mathrm{eq})}(t)]^2$, $\rho_w^{(\mathrm{eq})}(t)$, and $\rho_{w3}^{(\mathrm{eq})}(t)$ in Fig. 4. These three functions should agree with each other if $\mathbf{r}(t)$ is a Gaussian process. However, their time developments are different in the intermediate and the underdamped cases [Figs. 4(b) and 4(c)], which clearly indicates that $\mathbf{r}(t)$ does not belong to the Gaussian process. Since the relaxation time in the case of $\omega=1$ is much larger than the Enskog collision time, $\mathbf{r}(t)$ approaches the Gaussian process due to the central limiting theorem. In the cases of $\omega=3$ and 5, the relaxation of the width is slower than that of the average, which happens to agree with the experiments of Nishiyama and Okada. We consider that the slower relaxation of the width in our system is explained by the fact that, since all the relaxation rates are limited by the collision frequency (no relaxation can occur without collision), the relaxation of higher-order cumulants cannot become as fast as expected from the Gaussian assumption. The relaxation of the three-dimensional distribution is slower than that of one-dimensional distribution, which indicates the correlation between different components of $\mathbf{r}(t)$.

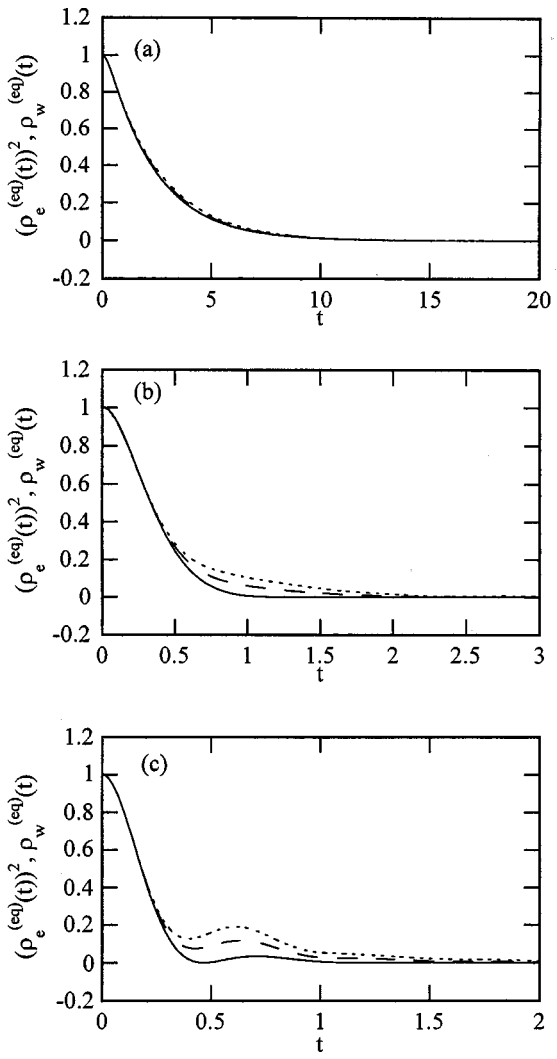

FIG. 4. Equilibrium time correlation functions of a tagged particle in a harmonic well. The solid, broken, and dotted curves are $\{\rho_e^{(\mathrm{eq})}(t)\}^2$, $\rho_w^{(\mathrm{eq})}\times(t)$, and $\rho_{w3}^{(\mathrm{eq})}(t)$, which are defined as Eqs. (12)–(14), respectively. The frequencies of the well are 1, 3, and 5 for (a), (b), and (c), respectively.

Hereafter we show the numerical results on the nonequilibrium relaxation of the tagged particle in the harmonic well. In Fig. 5, we show typical examples of the time development of the probability distribution. Both figures are the results of $\omega=3$, with different initial positions (x_0). Figures 5(a) and 5(b) are the results of $\omega x_0=0$ and 3, respectively. The former corresponds to the transient hole-burning spectrum near the absorption maximum, and the latter corresponds to the transient fluorescence spectrum with large solvation reorganization energy. The relaxation of distribution width shows rather complicated behavior in these figures. The width once becomes larger than the equilibrium one in Fig. 5(b), whereas such behavior is not found in Fig. 5(a). In Figs. 6 and 7, we show the relaxation function of distribution centers and widths defined as below:

$$\rho_e^{(\mathrm{ne})}(t)\equiv\frac{\langle x(t)\rangle_{\mathrm{ne}}}{\langle x(0)\rangle_{\mathrm{ne}}}, \tag{15}$$

$$\rho_w^{(\mathrm{ne})}(t)\equiv\frac{\langle(x(t)-\langle x(t)\rangle_{\mathrm{ne}})^2\rangle_{\mathrm{ne}}-\langle(x-\langle x\rangle_{\mathrm{eq}})^2\rangle_{\mathrm{eq}}}{\langle(x(0)-\langle x(0)\rangle_{\mathrm{ne}})^2\rangle_{\mathrm{ne}}-\langle(x-\langle x\rangle_{\mathrm{eq}})^2\rangle_{\mathrm{eq}}}, \tag{16}$$

Downloaded 06 Mar 2008 to 130.54.110.22. Redistribution subject to AIP license or copyright; see http://jcp.aip.org/jcp/copyright.jsp

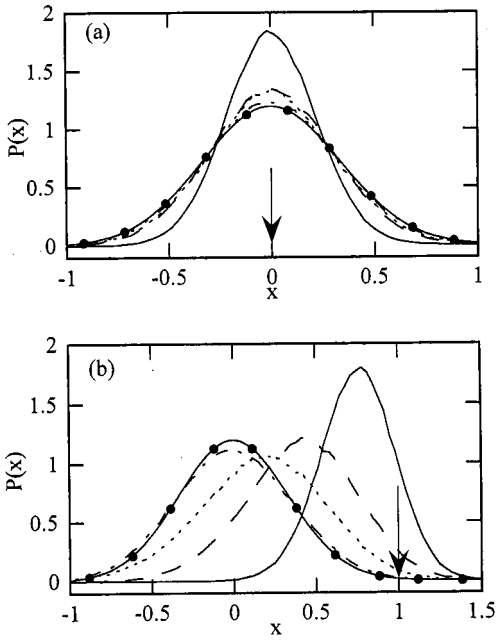

FIG. 5. The nonequilibrium spatial distributions of the tagged particle in the harmonic well whose frequency equals 3. Solid, broken, dotted, and dash-dotted curves are the distributions at $t=0.3$, 0.6, 0.9, and 1.5, respectively. The initial positions are 0 and 1 for (a) and (b), which are indicated by vertical arrows in the figure. Solid curves with filled circles are the equilibrium Gaussian distribution.

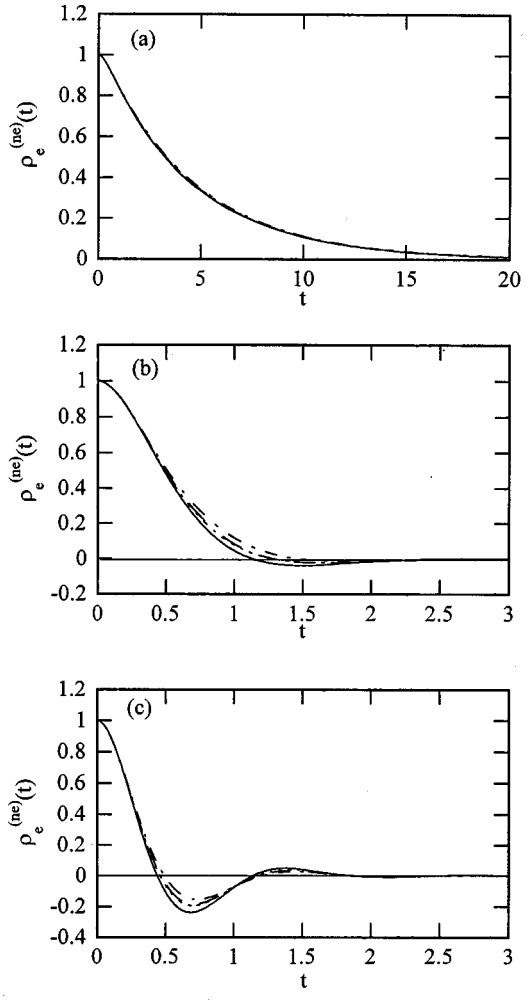

FIG. 6. The time development of the nonequilibrium relaxation function of the averaged position defined as Eq. (15). Solid, dotted, and dash-dotted curves are the relaxation functions when the initial positions are ω^{-1}, $2\omega^{-1}$, and $3\omega^{-1}$, respectively. Broken curves are the corresponding equilibrium time correlation function [Eq. (12)]. The frequencies of the well are 1, 3, and 5 for (a), (b), and (c), respectively.

where δU in Eqs. (2) and (3) is replaced by x in Eqs. (15) and (16). Looking at Fig. 6, it is noticed that the linear response assumption [Eq. (4)] works approximately well, and the agreement becomes better with a decrease of the frequency of the harmonic well. Deviations from the linear response are found for the wells of higher frequencies, and there is a tendency that the oscillation becomes smaller with an increase of the deviation of the initial position from the equilibrium one.

Figure 7 shows the relaxation function of the distribution width. Compared with Fig. 6, the deviation from the linear response [Eq. (5)] is larger than the case of distribution centers. As is the case in Fig. 6, the deviation becomes larger with an increase of the frequency of the well. In addition, the relaxation functions get smaller than zero when the value of x_0 and the frequency of the well are large, which corresponds to the broadening of distribution in Fig. 5(b). We do not have any explanation at present for the nonlinear response as is seen in Figs. 6 and 7. Since the collisional dynamics contains complex behavior even in the absence of correlation between collisions, the situation will be more complicated in liquids where many-body correlation is essential.

IV. CONCLUDING REMARKS

We have calculated nonlinear time correlated functions of a tagged particle in a dilute hard-sphere gas. In the absence of external forces on the tagged particle, the spatial distribution of the tagged particle broadens with an increase of time, and the transient distribution does not follow a Gaussian function. From the time development of the non-Gaussian parameter, we found that the non-Gaussian distribution lasts about 500 times as long as the Enskog collision time. This behavior is in parallel with those of Lennard-Jones liquids[2,3] and molten salts.[3] Therefore we consider that the liquid state dynamics has inherited its non-Gaussian character from the collisional dynamics of dilute gases.

We have also simulated the ''solvation dynamics'' in the dilute hard-sphere gas by trapping the tagged particle in a harmonic well. Both the equilibrium and the nonequilibrium time correlation functions are obtained. In the equilibrium runs, the relaxation of the distribution width is slower than that of the average, as is observed in the hole-burning experiments by Nishiyama and Okada. In the nonequilibrium runs, the linear response assumption works better for the distribution average than for the distribution width. The deviations from both Gaussian statistics and the linear response become larger with an increase of the frequency of the harmonic well. This indicates that the Gaussian statistics does not hold when the number of collisions is small. We suspect that such a non-Gaussian relaxation will be found in the ultrafast sol-

Downloaded 06 Mar 2008 to 130.54.110.22. Redistribution subject to AIP license or copyright; see http://jcp.aip.org/jcp/copyright.jsp

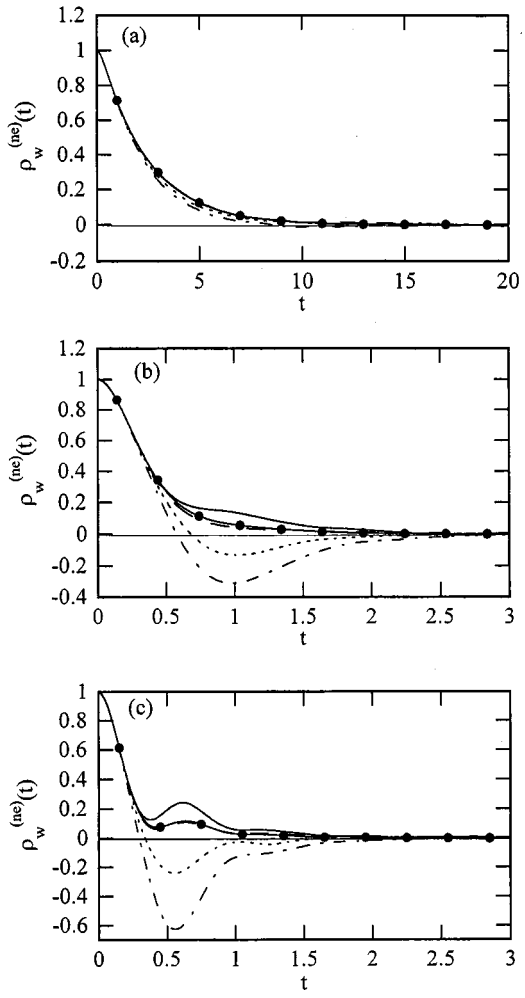

FIG. 7. The time development of the nonequilibrium relaxation functions of the distribution width defined as Eq. (16). Solid, broken, dotted, and dash-dotted curves are the relaxation when the initial positions are 0, ω^{-1}, $2\omega^{-1}$, and $3\omega^{-1}$, respectively. Solid curves with filled circles denote the corresponding equilibrium time correlation function [Eq. (13)]. The frequencies of the well are 1, 3, and 5 for (a), (b), and (c), respectively.

vation dynamics that is comparable with the collision frequency of liquids.

ACKNOWLEDGMENTS

We are grateful to Professor A. Morita (University of Tokyo) for useful discussion and comments on this manuscript. T.Y. gratefully acknowledges a research fellowships from the Japan Society for the Promotion of Science (JSPS) for Young Scientists.

APPENDIX: THE IMPLEMENTATION OF THE RANDOM WALK IN THE MOMENTUM SPACE DESCRIBED BY EQ. (8)

In our Monte Carlo calculation, we have used the finite difference method on the time axis in order to obtain the trajectory according to the transition probability of Eq. (8). Equation (8) can be transformed into the following form in the polar coordinate whose principal axis (z-axis) is parallel to $\mathbf{v}$:

$$
\begin{aligned}
&P_c(\mathbf{v},d\mathbf{v})d^3(d\mathbf{v})\Delta t \\
&= \frac{1}{\sqrt{2\pi}dv}\exp\left[-\frac{(dv+v\cdot\cos\theta)^2}{2}\right] \\
&\quad\times(dv)^2\sin\theta d(dv)d\theta\, d\varphi\,\Delta t \\
&= \left\{\frac{d(\cos\theta)}{2}\right\} \\
&\quad\times\left\{\frac{1}{\sqrt{2\pi}}\exp\left[-\frac{(dv+v\cdot\cos\theta)^2}{2}\right]d(dv)\right\} \\
&\quad\times\{4\pi dv\,\Delta t\}\left\{\frac{d\varphi}{2\pi}\right\},
\end{aligned}
\tag{A1}
$$

where $v=|\mathbf{v}|$, and $d\mathbf{v}=(dv\sin\theta\cos\varphi, dv\sin\theta\cos\varphi, \times dv\cos\theta)$. In Eq. (A1), all the units are scaled so that $\rho\sigma^2$, m, and k_BT are unity. In the case of free particle, the velocity at $t+\Delta t$ is determined from that at t with the following procedure. Firstly, $\cos\theta$ is determined to obey the uniform distribution between -1 and 1. Secondly, we generate dv as the Gaussian distribution whose average is $-v\cos\theta$ and whose variance is unity. The minus value of dv means that no collision occurs between t and $t+\Delta t$. Thirdly, the uniform distribution between 0 and 1 is generated, whose value is called p hereafter. A collision occurs when the value of p is smaller than $4\pi\, dv\,\Delta t$. Then, the value of φ is determined as the uniform distribution. The time of collision (t_c) follows the uniform distribution between t and $t+\Delta t$. The value of Δt is 0.0001 in all calculations. We performed several runs with different values of Δt to find that its effect is small.

In the case of trapped particles, we integrate the equation of motion with the following method:

$$
\begin{aligned}
\mathbf{v}(t+\Delta t) &= \mathbf{v}(t)\cos\omega\Delta t-\omega\mathbf{r}(t)\sin\omega\Delta t \\
&\quad + d\mathbf{v}\cos\omega(t+\Delta t-t_c),
\end{aligned}
\tag{A2}
$$

$$
\begin{aligned}
\mathbf{r}(t+\Delta t) &= \frac{\mathbf{v}(t)}{\omega}\sin\omega\Delta t+\mathbf{r}(t)\cos\omega\Delta t \\
&\quad + \frac{d\mathbf{v}}{\omega}\sin\omega(t+\Delta t-t_c).
\end{aligned}
\tag{A3}
$$

[1] K. Tominaga and K. Yoshihara, J. Phys. Chem. A **102**, 4222 (1998).
[2] A. Rahman, Phys. Rev. A **2**, 405 (1964).
[3] K. Itagaki, M. Goda, and H. Yamada, Physica A **265**, 97 (1999).
[4] K. Nishiyama and T. Okada, J. Phys. Chem. A **101**, 5729 (1997).
[5] T. Yamaguchi, J. Chem. Phys. **112**, 8530 (2000).
[6] J. Kielson and J. E. Storer, Quarterly Appl. Math. **10**, 243 (1952).
[7] G. Lévi, J. P. Marsault, F. Marsault-Hérail, and R. E. D. McClung, J. Chem. Phys. **73**, 2443 (1980).
[8] A. P. Blokhin and M. F. Gelin, Mol. Phys. **87**, 455 (1996).
[9] K. Andersen and K. E. Shuler, J. Chem. Phys. **40**, 633 (1964).
[10] J. O. Hirschfelder, C. F. Curtiss, and R. B. Bird, *Molecular Theory of Gases and Liquids* (Wiley, New York, 1954), Chap. 8.
[11] J.-P. Hansen and I. R. McDonald, *Theory of Simple Liquids*, 2nd ed. (Academic, London, 1990).
[12] See, e.g., A. Papoulis, *Probability, Random Variables, and Stochastic Processes* (McGraw-Hill, New York, 1984).

Downloaded 06 Mar 2008 to 130.54.110.22. Redistribution subject to AIP license or copyright; see http://jcp.aip.org/jcp/copyright.jsp